2016 International Symposium on Nonlinear Theory and Its Applications,
NOLTA2016, Yugawara, Japan, November 27th-30th, 2016

On Smoothing Effects of Wind Power Via Koopman Mode Decomposition

Fredrik Raak†, Yoshihiko Susuki‡, Kazuhisa Tsuboki§, Masaya Kato§, and Takashi Hikihara†

†Department of Electrical Engineering, Kyoto University
Nishikyo, Kyoto 615–8510, Japan
‡Department of Electrical and Information Systems, Osaka Prefecture University
1–1 Gakuen-cho, Naka-ku, Sakai, Osaka 599–8531, Japan
§Hydrospheric-Atmospheric Research Center, Nagoya University
Chikusa, Nagoya 464–8601, Japan
Email: f-raak@dove.kuee.kyoto-u.ac.jp

Abstract—In this paper we apply a method known as Koopman Mode Decomposition (KMD) to data on simulated wind power outputs. We propose a new index which characterizes the smoothing of total output from multiple wind turbines or farms, through the spectral decomposition achieved via KMD. The index is experimentally exemplified via application to data where the maximum distance between measurement locations ranges from kilometers to hundreds of kilometers. Data on wind speeds from weather predictions obtained with CReSS (Cloud-Resolving Storm Simulator) are used together with a standard power curve to simulate outputs of wind turbines/farms. Results show that KMD reconstructs the wind farm output well by a set of modes, and that the smoothing resembles the conventional index based on power spectral densities for some cases. Furthermore, it is demonstrated with the KMD-based index that the smoothing on hour-scale for distributed wind farms in Japan exhibits similarity to the improved smoothing observed by distributing turbines over a larger area in a wind farm.

1. Introduction

In a system with large penetration of electric power from intermittent energy sources such as wind, it is important to distribute the generation over a large geographical area to smoothen the total power generation. It thus becomes important to quantify the coherence of power generation at different locations when planning a suitable distribution of renewable power generation.

Here we will look at the smoothing of aggregated wind power, which has previously been addressed in e.g. [1–3]. In particular, [1] describes a way to estimate the Fourier spectrum of the total output of multiple turbines via the spectrum of a single one. Smoothing of output power from a Wind Farm (WF) through Power Spectral Densities (PSD) is also discussed in [2], where the authors analyzed data in Japan. In [3], a statistical analysis of correlation between wind power is conducted on very large scale, where it is shown that the correlation between aggregate wind power of large systems is similar to that of correlation between WFs.

In this paper, we look at the smoothing of wind power on different spatial and temporal scales by incorporating more and less detailed data on wind speeds from CReSS (Cloud-Resolving Storm Simulator) [4]. The detailed 0.5 Hz sampled data with a spatial resolution of 200 m are obtained in an area outside the coast of Aomori Prefecture in northern Honshu, Japan, while the more coarse 1 h^{-1} sampled data with 2 km resolution in Japan. To analyze the smoothing effects of wind power, we apply the so-called Koopman Mode Decomposition (KMD) (from its connection to the *Koopman* operator in dynamical systems theory) [5] to output powers of Wind Turbines (WT) or WFs, which transforms the time-series data into a finite number of modes evolving with single frequencies.

The contributions of this paper are mainly two-fold. First, a new and easily applicable index for the smoothing effects of wind power is proposed and compared with a conventional one, e.g. [2]. Second, it newly looks at the application of large-scale weather simulation data to analyze smoothing effects of wind power in Japan, which could be a viable method of analyzing potential sites for large-scale wind power development in the future.

2. Conventional Index of Wind Power Smoothing

This section revisits a conventional index of wind power smoothing [6]. We let $S'(f)$ represent the PSD of wind speed at one WT in a WF, assuming that all WTs experience the same mean wind, and $\gamma_{ij}^2(f) = \exp(-a\frac{d_{ij}}{U}f)$ a function describing the coherency of wind speeds at the two measurement locations labeled by integers i and j that are separated by the distance d_{ij}, where a is a decay constant, U mean wind speed, and f frequency. Note that the exponential function is an approximation of coherence for turbulence used in micrometeorology [6]. Thus, when considering a collective effect of winds over the WF with N turbines, the PSD of time-varying component of collective wind speed is described in [6] as follows:

$$S_{\mathrm{WF}}(f) = S'(f)\frac{1}{N^2}\sum_{i=1}^{N}\sum_{j=1}^{N}\gamma_{ij}(f), \qquad (1)$$

where $\frac{1}{N^2}\sum_{i=1}^{N}\sum_{j=1}^{N}\gamma_{ij}(f)$ is called the WF filter, which depends on the coherence functions and quantifies the degree of smoothing achieved at the WF.

Now considering wind power instead, the PSD of output power P_{WF} at a WF can be approximated in [2] as follows:

$$S_{P_{\text{WF}}}(f) = S'_P(f)\sum_{i=1}^{N}\sum_{j=1}^{N}\Gamma_{ij}(f)\cos(\phi_{ij}(f)), \quad (2)$$

similar to (1), where $S'_P(f)$ represents the PSD of output power at a typical WT, $\phi_{ij}(f)$ a function determining the phases of power outputs, and Γ_{ij} the coherence function. The WF filter here becomes $G_{\text{WF}}(f) := S_{P_{\text{WF}}}(f)/S'_P(f) = \frac{1}{N^2}\sum_{i=1}^{N}\sum_{j=1}^{N}\Gamma_{ij}(f)\cos(\phi_{ij}(f))$. The coherence function $\Gamma_{ij}(f)$ is in [2] as follows:

$$\Gamma_{ij}(f) = \frac{|S_{P_{ij}}(f)|}{\sqrt{S_{P_{ii}}(f)S_{P_{jj}}(f)}}, \quad (3)$$

which quantifies the magnitude of overlapping frequency content of two signals, where $S_{P_{ii}}$ is the PSD of electric power at WT i, and $S_{P_{ij}}$ the cross spectral density between i and j. It is shown in [2] that the exponential approximation of (3) like above offers a good agreement with experimentally-obtained data in Japan.

Suppose that output powers P_i are measured at every WT i, and the total power corresponds to $P_{\text{tot}} = \frac{1}{m}\sum_{i=1}^{m}P_i$ in per unit (p.u.). The following smoothing index with respect to a "typical" WT i is then derived:

$$s_i(f) := \sqrt{S_{P_{\text{tot}}}(f)/(S_{P_i}(f))}, \quad (4)$$

which is the gain of $G_{\text{WF}}(f)$ in accordance with [2], as a comparison to (9) proposed later for KMD. The functions $S_{P_{\text{tot}}}$ and S_{P_i} are the PSDs of P_{tot} and P_i. Since a "typical WT" could be a difficult task to determine, in particular when outputs and locations vary significantly, we consider calculating the mean smoothing according to

$$s(f) := \texttt{tmean}(s_i(f)), \quad (5)$$

where `tmean` represents the 25 % truncated mean over all WTs $i = 1, \ldots, m$, to remove outliers.

3. New Smoothing Index via Koopman Modes

In this section, we introduce a new index to characterize the smoothing effects of wind power based on the so-called Koopman Mode Decomposition (KMD). We refer to [5, 7–9] for detailed theoretical background of KMD.

Now, we consider $N+1$ vector-valued snapshots of wind power measurements collected at m locations: $\{\boldsymbol{P}_0, \ldots, \boldsymbol{P}_N\}$, $\boldsymbol{P}_k \in \mathbb{R}^m$. The sampled time-series are then decomposed into a finite sum via KMD:

$$\left.\begin{aligned}\boldsymbol{P}_k &= \sum_{i=1}^{N}\tilde{\lambda}_i^k\tilde{\boldsymbol{v}}_i, \quad k = 0, \ldots, N-1,\\ \boldsymbol{P}_N &= \sum_{i=1}^{N}\tilde{\lambda}_i^N\tilde{\boldsymbol{v}}_i + \boldsymbol{r},\end{aligned}\right\} \quad (6)$$

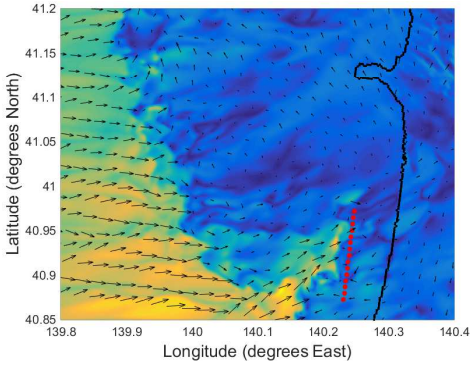

Figure 1: Placement of wind turbines (red dots) in a hypothetical wind farm with 600 m distance between turbines. The colored background and arrows indicate the speed and direction of wind. The black curve depicts the coastline of Aomori Prefecture.

computed via an Arnoldi-type algorithm [5], giving N pairs of so-called Ritz-values $\tilde{\lambda}_i \in \mathbb{C}$ and vectors $\tilde{\boldsymbol{v}}_i \in \mathbb{C}^m$. The vector $\boldsymbol{r}$ is the residual component in KMD; if assumed to be zero, (6) becomes

$$\boldsymbol{P}_k = \sum_{i=1}^{N}\tilde{\lambda}_i^k\tilde{\boldsymbol{v}}_i, \quad k = 0, \ldots, N. \quad (7)$$

Frequencies are calculated as $f_i = \text{Im}(\ln(\tilde{\lambda}_i))/(2\pi T_s)$, where T_s is the sampling period of data. The vector $\tilde{\boldsymbol{v}}_i$ is here called the Koopman Mode (KM) and contains the magnitudes and phases of power fluctuations at the measurement locations for the frequency f_i. To identify lightly damped or undamped oscillations with large magnitude, all N KMs are sorted by $(\tilde{\lambda}_i)^N\|\tilde{\boldsymbol{v}}_i\|$, and higher ranked ones are called *dominant* KMs. Here, KMD will be applied to wind powers at m locations, representing hypothetical WTs or WFs. The total power $P_{\text{tot},k}$ can be expressed using (7) as

$$P_{\text{tot},k} = \sum_{i=1}^{N}\tilde{\lambda}_i^k\sum_{j=1}^{m}[\tilde{\boldsymbol{v}}_i]_j = \sum_{i=1}^{N}\tilde{\lambda}_i^k\overline{\boldsymbol{v}}_i, \quad (8)$$

where $\overline{\boldsymbol{v}}_i \in \mathbb{C}$ is the scalar KM of the total output. That is, a spectral decomposition of the total output power is achieved through the decomposition of individual outputs. Now let $\overline{A}_i = |\overline{\boldsymbol{v}}_i|$ be the amplitude factor the i-th KM oscillation for the total output, and analogously $A_{ij} = |\boldsymbol{v}_{ij}|$ the factor for the same oscillation for a WT or WF j, and $\boldsymbol{A}_i = [A_{i1}, \ldots, A_{im}]^\top$ ($\top$ denotes vector transpose.) Then we define

$$s_i := \overline{A}_i/(m \cdot \texttt{tmean}(\boldsymbol{A}_i)), \quad (9)$$

as a index of smoothing with respect to frequency f_i, where `tmean` is same as in (5), taken over all m turbines, and m is included in (9) to scale down the total output to p.u. If the amplitude of an oscillation is smaller in the sum than for individual WTs or WFs, then (9) becomes smaller than one for that particular f_i.

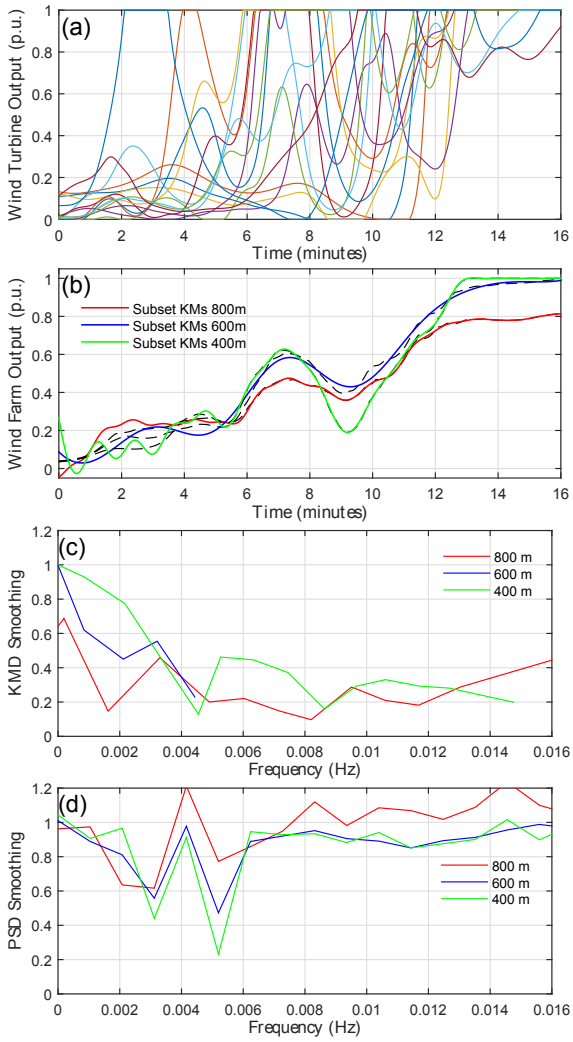

Figure 2: (a) Turbine outputs for 600 m (distance between consecutive turbines) case; (b) wind farm outputs and approximations by dominant KMs; smoothing results via (c) KMD and (d) PSDs.

4. Demonstration

Now, two examples are used to evaluate the index proposed in this paper. The first one incorporates 0.5 Hz sampled wind prediction data from the CReSS weather model [4], averaged over a grid with 200 m spatial resolution. The data are used as input to WTs in a hypothetical WF outside the coast of Aomori Prefecture in Japan [10]. A single array of 15 turbines is considered, and three cases are considered where the distances between consecutive turbines are chosen as 400, 600, and 800 m; see red dots in Fig. 1 which depicts the 600 m case. The "lowest" WT position in the figure is common for all cases. Wind speeds are converted into power outputs with a standard power curve. The KMD and proposed index are applied to sampled powers for 16 minutes, where wind speeds are dramatically increasing due to an incoming winter storm, and turbine outputs are shown in Fig. 2 (a) for the 600 m case.

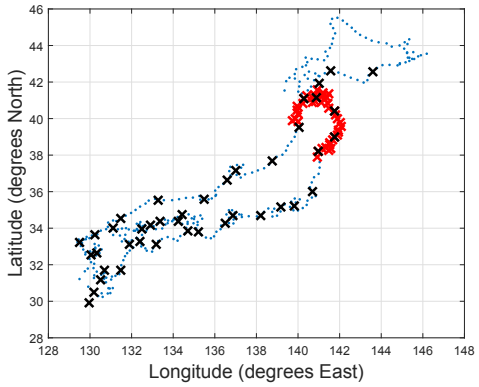

Figure 3: Measurement points outlining the coasts of Japan's main islands. The red crosses indicate a case of concentrated wind power production (Case 1) and black crosses the case of most sparsely distributed (Case 5).

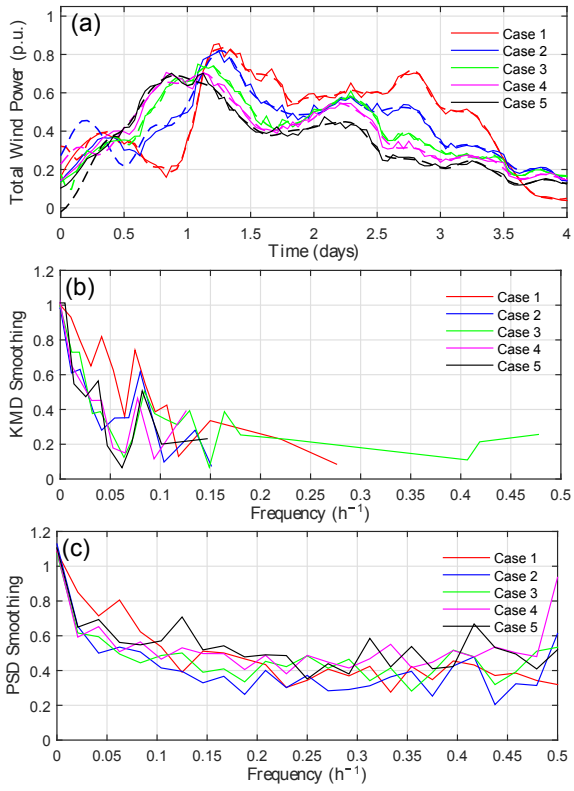

Figure 4: (a) Aggregated wind farm outputs depicted by solid curves and comparison with the reconstructed outputs by dominant KMs with the dashed lines; smoothing of wind power by (b) KMD and (c) PSDs.

Fig. 2 (b) shows how well the subsets of dominant KMs approximate the wind farm outputs using (8). Smoothing results for all cases calculated with (9) are presented in Fig. 2 (c). The results indicate considerable smoothing that increases with higher frequency. In particular, for frequencies higher than about $4 \cdot 10^{-3}$ Hz, i.e. periods less than 4 min, s_i becomes small, indicating the wind farm smooth-

ing. As a comparison, the smoothing index $s(f)$ calculated via PSDs is given in Fig. 2 (d). The results on PSD-based smoothing initially looks similar and then increases towards and *above unity* for all cases. This would imply that a certain fluctuation in the output of a WT is magnified by the wind farm, which is not realistic. If all WTs e.g. oscillate 1 p.u. in unison for a particular frequency, the wind farm output would also oscillate with 1 p.u. (with respect to its maximum capacity.) The issue here may be that the different WTs have significantly different spectrum, thus it becomes difficult to average the results or estimate the smoothing based on a single turbine output.

On the other hand, the KMD-based smoothing result indicates that the smoothing significantly improves for the 800 or the 600 m distance case between WTs compared with the 400 m case, in difference to the PSD-based index which is inconclusive on this point. We see that this seems to agree with the observed WF outputs in Fig. 2 (b) since e.g. the WF output in the 800 m case fluctuates less than for the 400 m case.

Now we look at more coarse CReSS data of whole Japan (2 km spatial resolution and $T_{\mathrm{s}} = 1$ h). We consider 41 hypothetical wind farms (or locations) whose outputs are calculated with the same power curve used previously. The locations vary from a WF distribution concentrated to the northern part of Honshu (Case 1) to sparsely distributed WFs all along Japan's coastline (Case 5). The two most extreme cases (1 and 5) are shown in Fig. 3 and highlighted by red and black crosses. The total outputs of all wind farms for the all cases are given in Fig. 4 (a), together with the reconstructed outputs by dominant KMs, and smoothing results are given in Figs. 4 (b) and (c).

In this case, the KMD-based smoothing index shows more resemblance to the results achieved via PSD-based smoothing, although indicating slightly more smoothing. The cause of more resemblance here might be that the spectrum at different locations are more homogeneous, thus the smoothing based on the mean or individual PSDs become similar. According to the KMD-based smoothing, the improved smoothing on this large scale resembles the improvement achieved in the previous example for a WF (compare Fig. 2 (c) and Fig. 4 (c)), by distributing WTs over a larger area, however more data should be considered in the future to validate this. This scale invariability is also supported by the results of e.g. [3, 11]. In particular [11] shows that the reduced variability of summed power outputs of WFs is comparable to that of individual WFs.

5. Conclusions

A new smoothing index of aggregated wind power was proposed based on measurements of power at each wind farm or turbine, via the so-called Koopman Mode Decomposition. The index was applied to wind turbine outputs in a hypothetical wind farm in an area attractive for wind power in Japan, as well as to coarse data of whole Japan. According to the proposed index, the improved smoothing on hour-scale for distributed wind farms in Japan becomes similar to the improved smoothing by distributing turbines over a larger area in a wind farm. However, an investigation including more data should be conducted to validate the correctness of this, which is one of the future works. The KMD-based index and conventional power spectral density-based one become similar for one of two cases here. We speculate that the agreement is dependent on the degree of homogeneity of the spectrum of turbines and farms, which could make it difficult to average the smoothing result or select an appropriate comparison to the aggregated wind power output.

References

[1] G. McNerney and R. Richardson, "The statistical smoothing of power delivered to utilities by multiple wind turbines," *IEEE Transactions on Energy Conversion*, vol. 7, no. 4, pp. 644–647, 1992.

[2] T. Nanahara, M. Asari, T. Sato, K. Yamaguchi, M. Shibata, and T. Maejima, "Smoothing effects of distributed wind turbines. Part 1. Coherence and smoothing effects at a wind farm," *Wind Energy*, vol. 7, no. 2, pp. 61–74, 2004.

[3] H. Louie, "Correlation and statistical characteristics of aggregate wind power in large transcontinental systems," *Wind Energy*, vol. 17, no. 6, pp. 793–810, 2014.

[4] K. Tsuboki, "High-resolution simulations of high-impact weather systems using the cloud-resolving model on the Earth Simulator," in *High Resolution Numerical Modelling of the Atmosphere and Ocean*, pp. 141–156, Springer, 2008.

[5] C. W. Rowley, I. Mezić, S. Bagheri, P. Schlatter, and D. S. Henningson, "Spectral analysis of nonlinear flows," *Journal of Fluid Mechanics*, vol. 641, pp. 115–127, 2009.

[6] J. Manwell, J. McGowan, and A. Rogers, *Wind Energy Explained: Theory, Design and Application*. Wiley, 2009.

[7] I. Mezić, "Spectral properties of dynamical systems, model reduction and decompositions," *Nonlinear Dynamics*, vol. 41, no. 1-3, pp. 309–325, 2005.

[8] M. Budišić, R. Mohr, and I. Mezić, "Applied Koopmanism," *Chaos*, vol. 22, no. 4, 2012.

[9] I. Mezić, "Analysis of fluid flows via spectral properties of the Koopman operator," *Annual Review of Fluid Mechanics*, vol. 45, pp. 357–378, 2013.

[10] F. Raak, Y. Susuki, R. Morita, T. Wada, K. Tsuboki, H. Uyeda, Y. Fujisaki, and T. Hikihara in *Proceedings, IECON 2015 - 41th Annual Conference of the IEEE Industrial Electronics Society*, 2015.

[11] C. M. S. Martin, J. K. Lundquist, and M. A. Handschy, "Variability of interconnected wind plants: correlation length and its dependence on variability time scale," *Environmental Research Letters*, vol. 10, no. 4, p. 044004, 2015.